Supporting Information

Modeling the ionization efficiency of small molecules in positive electrospray ionization using molecular dynamics simulations

Dimitri Abrahamsson[1,2], Lelouda-Athanasia Koronaiou[3,4], Trevor Johnson[1], Junjie Yang[2], Xiaowen Ji[1] and Dimitra A. Lambropoulou[3,4]

[1] Department of Pediatrics, New York University Grossman School of Medicine, New York, New York 10016, United States

[2] Department of Obstetrics, Gynecology and Reproductive Sciences, School of Medicine, University of California, San Francisco, California 94158, United States

[3] Laboratory of Environmental Pollution Control, Department of Chemistry, Aristotle University of Thessaloniki, University Campus 54124 Thessaloniki, Greece

[4] Center for Interdisciplinary Research and Innovation (CIRI-AUTH), Balkan Center, Thessaloniki 57001, Greece

Contents: Text S1-S2, Figures S1-S10 and Tables S1-S2

*Corresponding author: Dimitri Abrahamsson, dimitri.abrahamsson@gmail.com

SUPPLEMENTARY TEXT

Text S1: Determining the number of H_3O^+ ions

We extracted the underlying data from the publication[1] using WebPlotDigitizer and reconstructed the figures from the extracted datapoints (Figure S2). The relationship between diameter and droplet charge was described by fitting a power trendline of the form of:

$$y = ax^b \quad \text{(eq. S1)}$$

In place of diameter, we used the body diagonal of the 64 nm^3 cube, calculated from:

$$D = \sqrt{3}a \quad \text{(eq. S2)}$$

which was determined to be 6.9 nm. The number of calculated H_3O^+ molecules in a droplet with a diameter of 6.9 nm was calculated to be 149 in a water droplet and 108 in a methanol droplet. Using the average of these two values we estimated 129 H_3O^+ molecules for our system. In order to verify whether this number is in agreement with other experimental observations and with electrochemical theory, we applied the Nernst equation to calculate the output voltage of a 64 nm^3 droplet with 129 H_3O^+ molecules and compared that to the observations of Maze et al.[2] For an electrochemical cell with water, where the following reactions take place:

$$2H_2O + 2e^- \rightleftharpoons H_2 + 2OH^- \quad \text{(eq. S3)}$$

$$2H^+ + 2e^- \rightleftharpoons H_2 \quad \text{(eq. S4)}$$

$$O_2 + 2H_2O + 4e^- \rightleftharpoons 4OH^- \quad \text{(eq. S5)}$$

$$O_2 + 4H^+ + 4e^- \rightleftharpoons 2H_2O \qquad \text{(eq. S6)}$$

the Nernst equation[3,4] for the half-reaction eq. S4 is as follows:

$$E = E^0 - \frac{0.059}{2} \log \frac{p(H_2)}{[H^+]^2} \qquad \text{(eq. S7)}$$

where, E is the cell potential (in our case the droplet potential), E^0 is the standard reduction potential, p is the pressure of the system.

For eq. S7, $E^0 = 0$,[3] and for our experiment, p = 1 atm, hence, eq. S7 can be written as

$$E = -\frac{0.059}{2} \log \frac{1}{[H^+]^2} \qquad \text{(eq. S8)}$$

Converting the number of 129 H^+ in 64 nm^3 to concentration we get 2 x 10^{24} H^+/L, which when converted to mol/L using Avogadro's number equals to 3.35 mol/L. Solving E in eq. S8 for $[H^+]$ 3.35 mol/L gives E = 0.031 V. Maze et al.[2] observed an output voltage of 0.5 V for a droplet with 4 µm diameter. Considering that our system is substantially smaller and given that Smith et al.[1] observed a decrease in charge with decreasing diameter, we concluded that our estimated number of 129 H_3O^+ is within a reasonable range.

Text S2: Determining the number of H+ ions

One of the challenges we faced during the simulations was that when using a small number of H^+ ions (e.g., 30), the ions moved towards the edges of the water droplet and did not sufficiently interact with the analyte that often remained in the center of the box (Figure S3 and S4). This may be hard to see in a 2D representation (Figure S3 and S4) but it can be clearly seen in the calculations of the Coulomb and Lennard-Jones interactions (Figure S5).

Both System 1 and System 2 were neutralized with the addition of OH^- ions equal to the number of $H3O^+$ for System 1 and to the number of H^+ for System 2. It should be noted that although, OH^- are not expected to be at such high concentrations in ESI+, neutralizing the system is necessary in order to conduct the simulations. Not neutralizing the system results in an unstable system that crashes before the simulation is completed. It should be clarified that although OH^- ions were added to the system, their interactions with the analyte were not included in the model for predicting RRF. It should also be noted that the addition of OH^- ions does not influence the interactions of the analyte with the water, methanol, $H3O^+$ and H^+ molecules. The interactions between the analyte and each group of molecules (e.g., water) are not dependent upon the interactions of the analyte and another group of molecules (e.g., OH^-).

SUPPLEMENTARY FIGURES

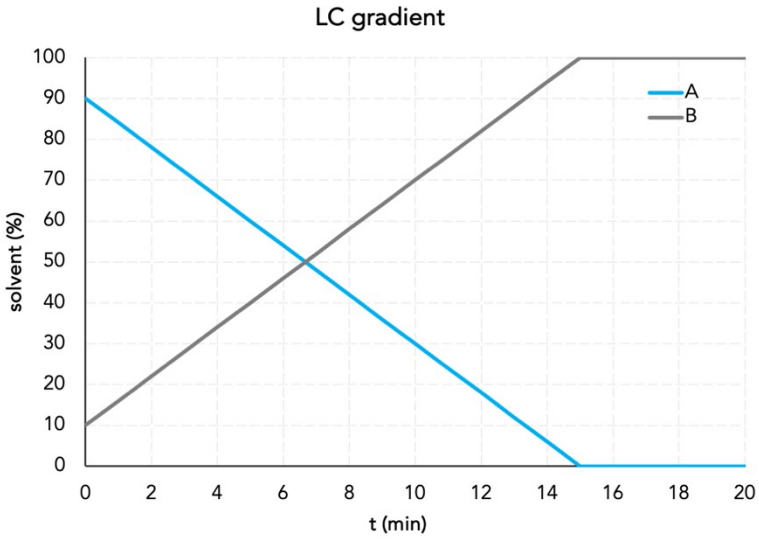

Figure S1: Liquid chromatography gradient showing the percentages of solvent A and B over time. A: HPLC water with 0.1% methanol and 5 mM ammonium acetate. B: methanol with 10% HPLC water and 5 mM ammonium acetate.

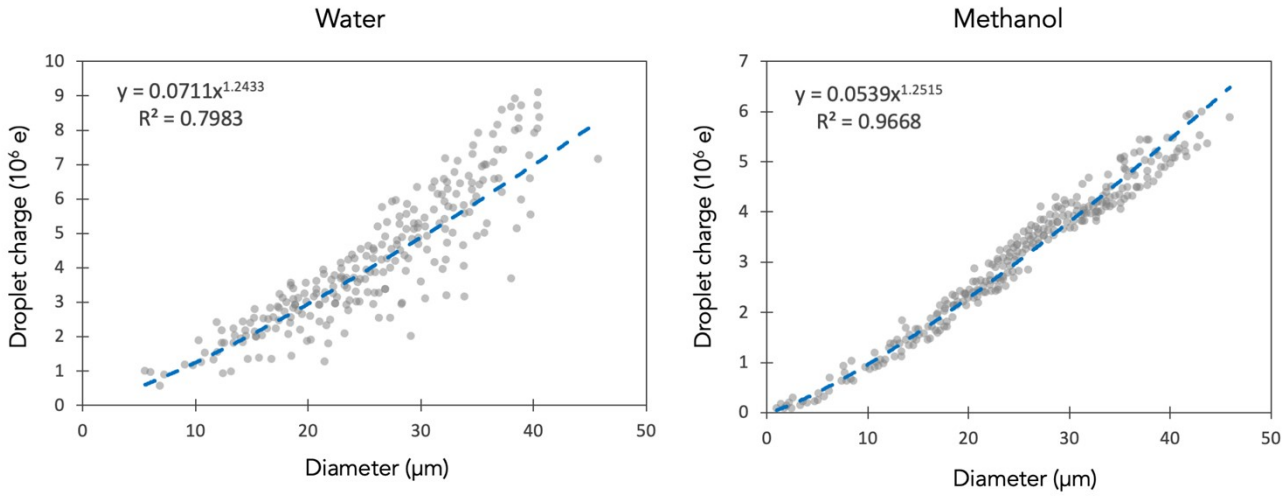

Figure S2: Reconstructed figures from the publication of Smith et al.[1] showing the relationship between charge and droplet diameter for electrospray droplets created in positive electrospray ionization for water and methanol. The trendline is shown in red. The number of calculated H_3O^+ molecules in a droplet with a diameter of 6.9 nm was calculated to be 149 in a water droplet and 108 in a methanol droplet.

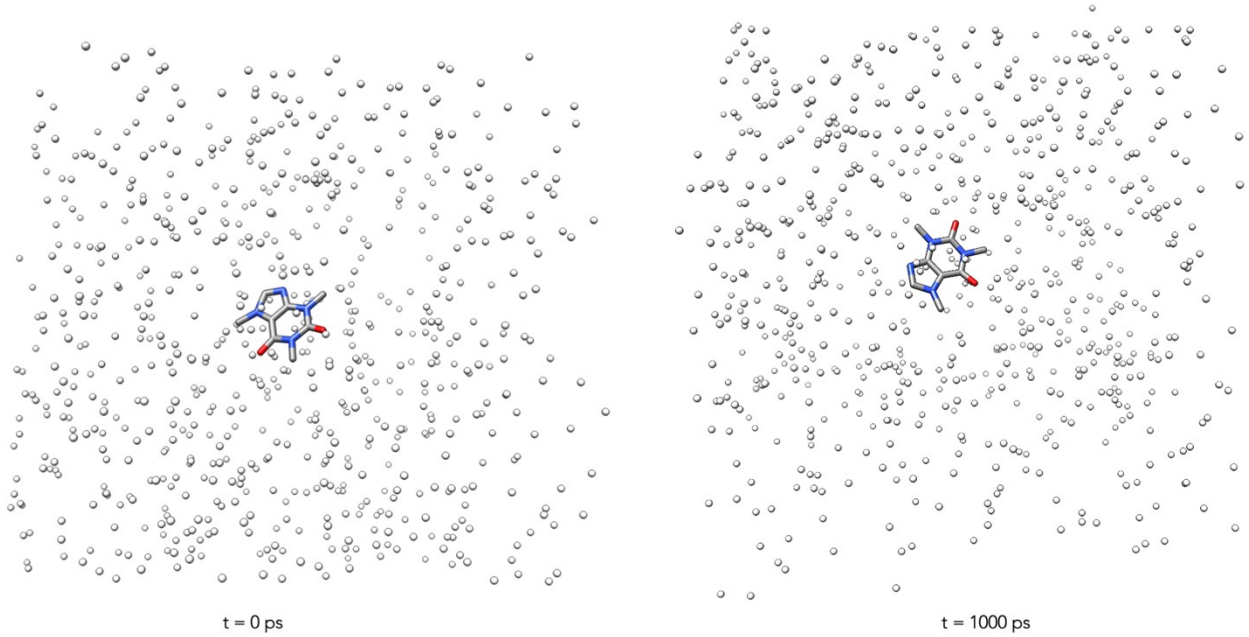

111

112 Figure S3: Caffeine in a solvent box among H^+ ions at t = 0 ps and at t = 1000 ps. The box contained 1

113 molecule of caffeine, 625 water molecules, 699 OH^- ions and 699 H^+ ions. The figure shows only the

114 caffeine molecule and the H^+ ions for simplicity.

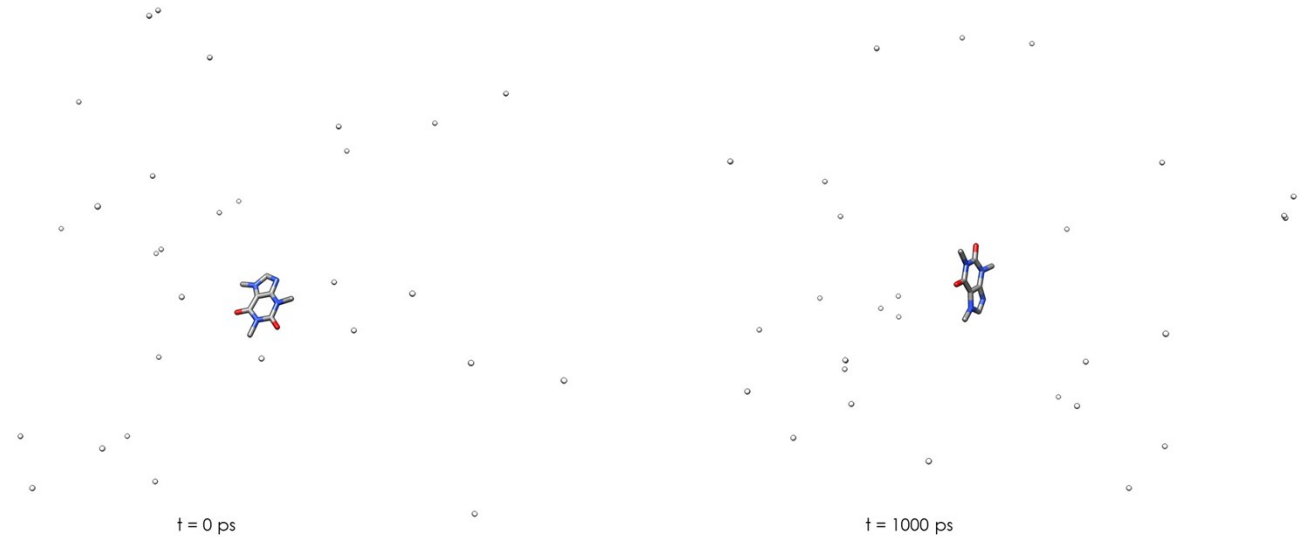

115

Figure S4: Caffeine in a solvent box with H^+ ions at t = 0 ps and at t = 1000 ps. The box contains 1 molecule of caffeine, 30 H^+ ions, 2084 water molecules and 30 OH^- ions. The figure shows only the caffeine molecule and the H^+ ions for simplicity.

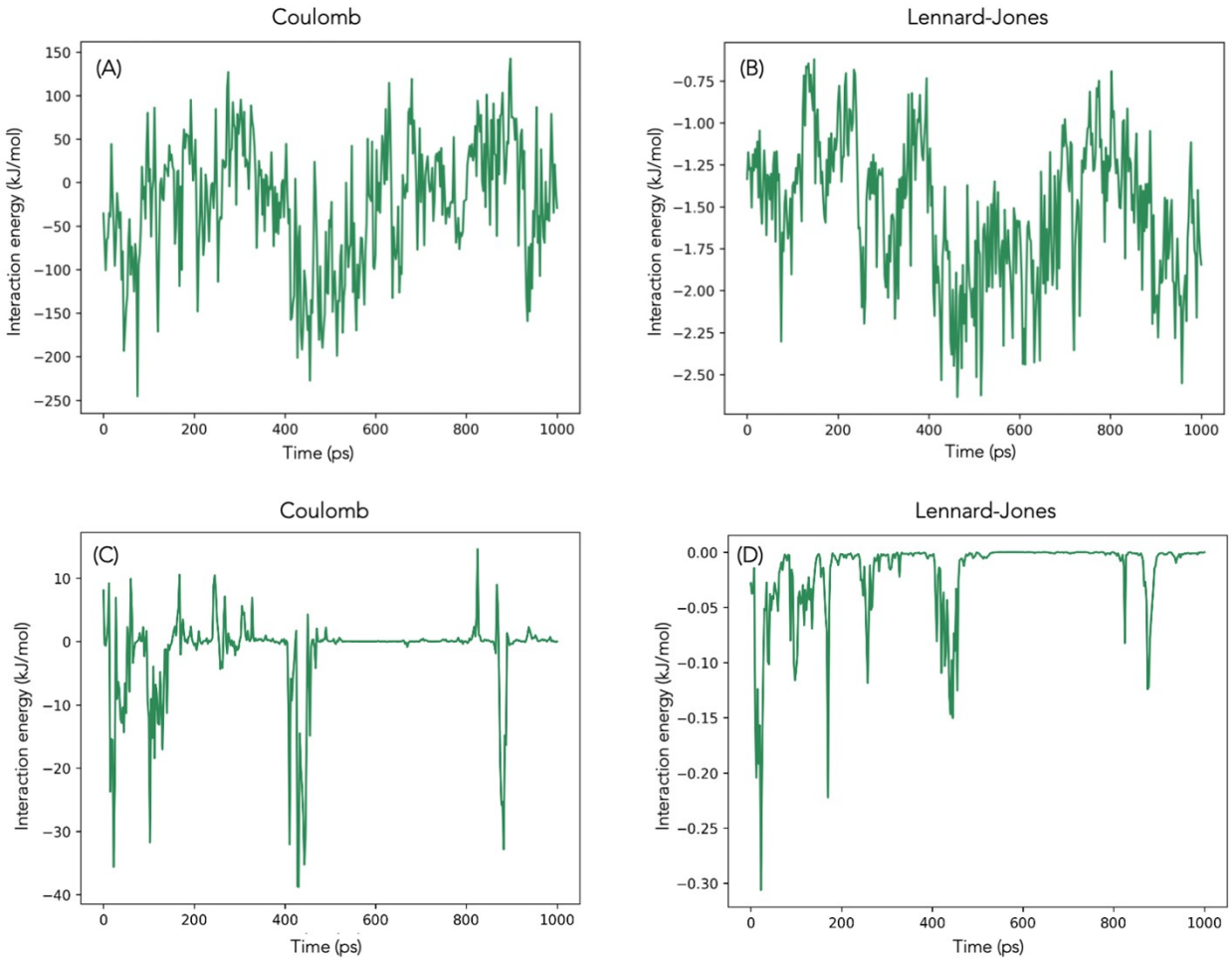

Figure S5: Coulomb and Lennard-Jones interactions between caffeine and H^+ ions during the simulation. The top figures (A and B) show the Coulomb and Lennard-Jones interactions over time for a system with 699 H^+ ions and the bottom figures show the interaction energies for a system with 30 H^+ ions.

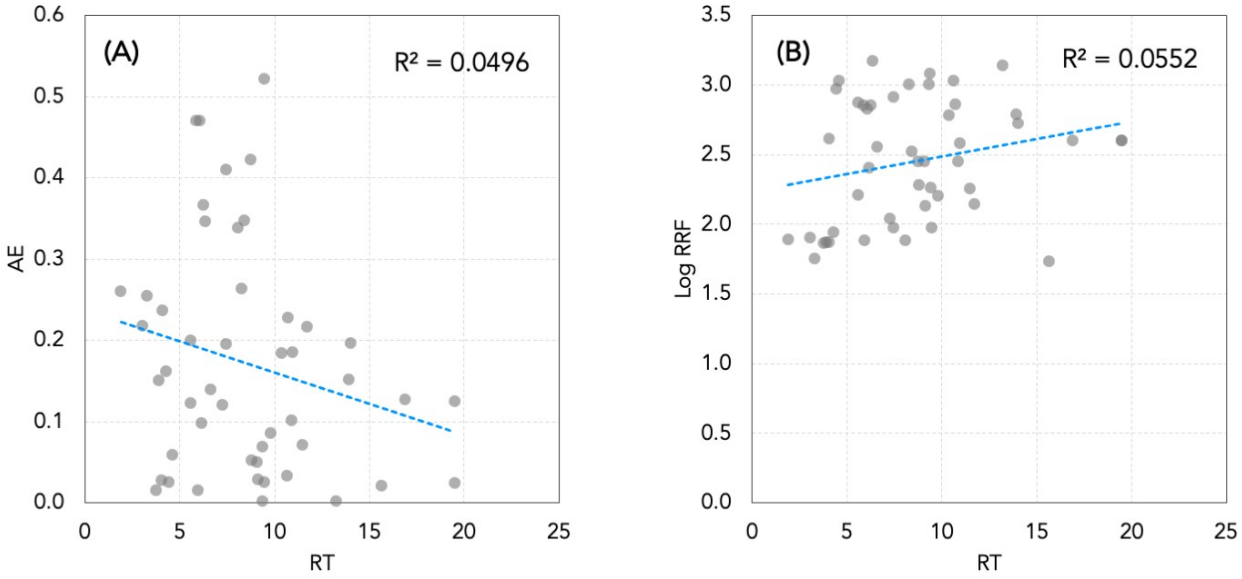

Figure S6: A: Relationship between the absolute errors (AE) of the model and retention time (RT). B: Relationship between RT and RRF.

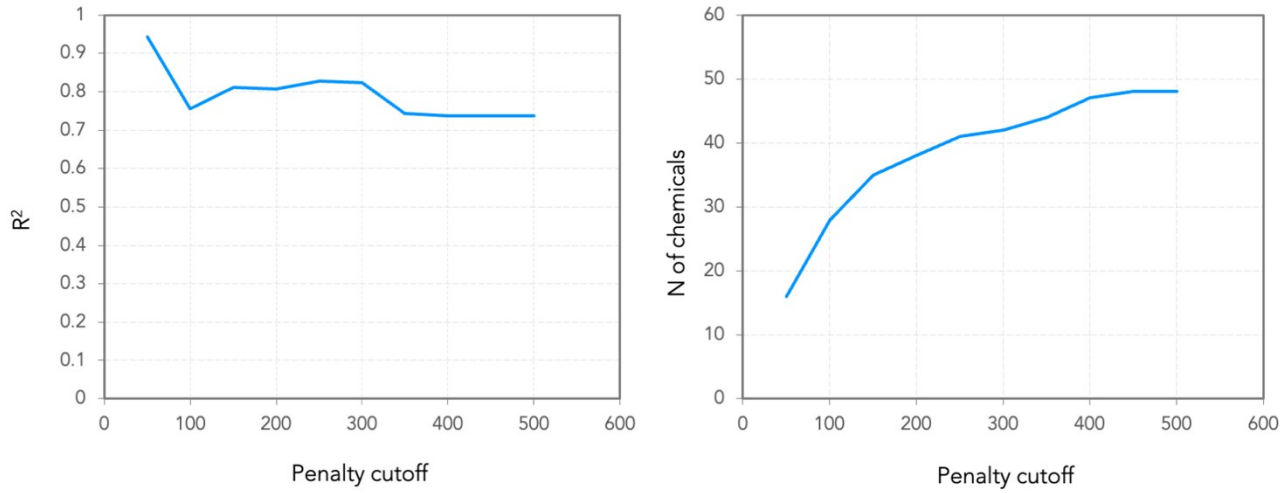

Figure S7: R^2 of the model and number of chemicals as a function of the penalty cutoff point for including chemicals in the dataset. As the penalty cutoff point decreases so does the number of chemicals included in the model. The R^2 of the model appears to be consistent with an increase around 300. At cutoff point 50 the model shows a high R^2 as a result of overparameterization given the small number of chemicals remaining in at this cutoff point (n=16).

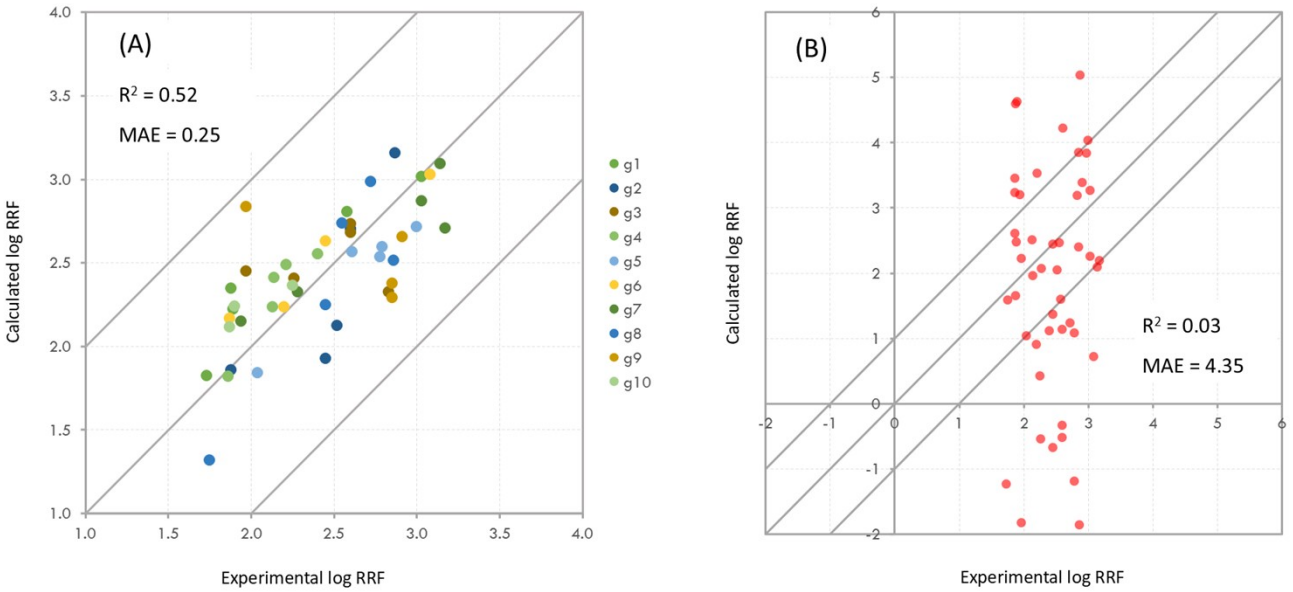

Figure S8: (A) 10-fold cross-validation showing the individual groups of compounds for each fold. The figure shows the results for each group of compounds when these compounds were not included in the training set. (B) Y-randomization for all the compounds in the dataset. R^2 is the coefficient of determination and MAE is the mean absolute error between the predictions and the experimental values.

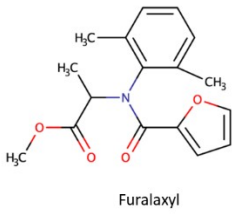

Furalaxyl

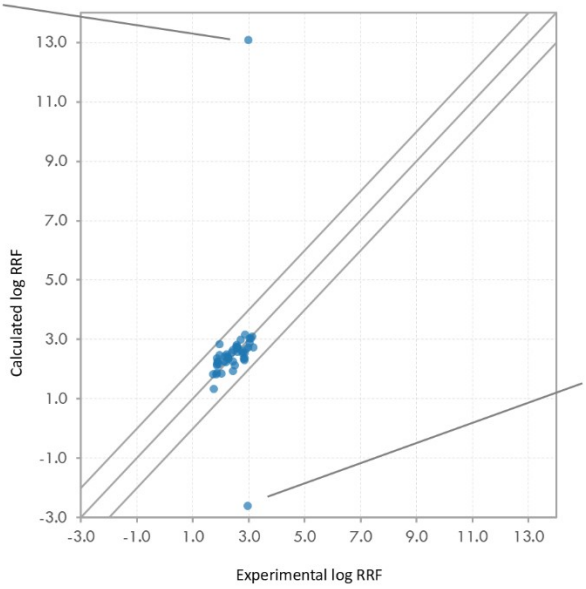

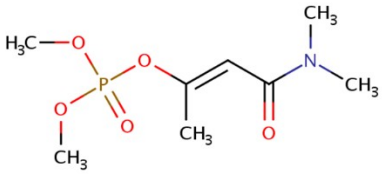

Dicrotophos

Figure S9: 10-fold cross-validation showing the results for the testing sets including the two outliers that were excluded for being outside the applicability domain of the models that were used to predict their log RRF. The figure shows the results for each group of compounds when these compounds were not included in the training set.

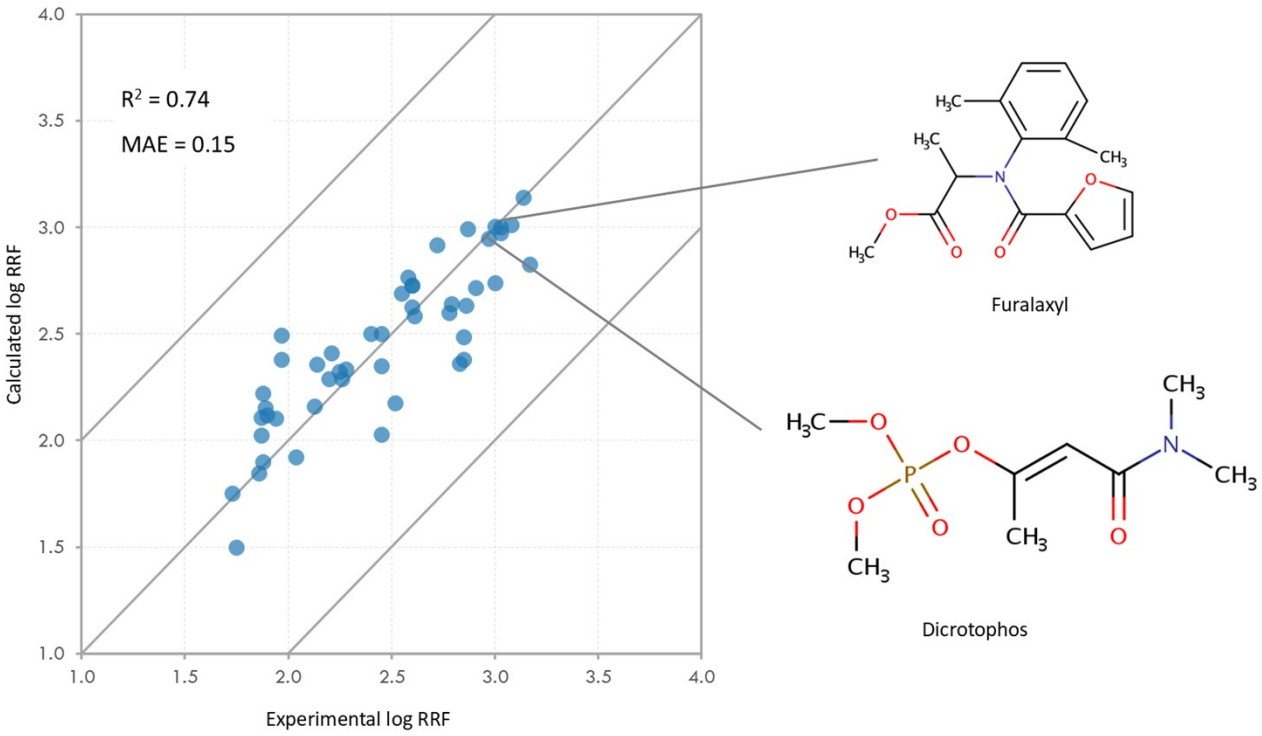

Figure: S10: Experimental and predicted values of log transformed RRF. The diagonal lines show the 1-to-1 agreement line, and the ± 1 log unit deviation line. The figure shows the results of the model including all the chemicals in the dataset and pointing the results for Furalaxyl and N,N-Dibutylthiourea.

SUPPLEMENTARY TABLES

Table S1: Statistics for the multi-parameter linear regression model that contained all compounds in the dataset

All compounds

R^2	0.74					
	coefficient	standard error	t	p-value	[0.025	0.975]
const	2.51	0.278	9.049	0.000	1.95	3.078
LJ_{p1}	0.53	0.328	1.607	0.117	-0.139	1.193
LJ_{p2}	-6.04	1.509	-4.001	0.000	-9.101	-2.974
LJ_{p3}	5.24	1.407	3.725	0.001	2.384	8.096
LJ_{std}	3.47	0.883	3.934	0.000	1.681	5.267
$Coul_{p1}$	-0.01	0.002	-3.421	0.002	-0.009	-0.002
$Coul_{p2}$	0.02	0.01	2.195	0.035	0.002	0.043
$Coul_{p3}$	-0.02	0.01	-1.705	0.097	-0.036	0.003
$Coul_{std}$	-0.03	0.007	-4.995	0.000	-0.048	-0.02
W LJ_{p2}	0.18	0.054	3.318	0.002	0.07	0.289
W LJ_{p3}	-0.17	0.055	-3.145	0.003	-0.284	-0.061
W LJ_{std}	0.31	0.082	3.761	0.001	0.143	0.477
S_W	0.11	0.071	1.6	0.119	-0.031	0.258

Table S2: Statistics for the multi-parameter linear regression model that contained compounds with a penalty less than 300

Compounds with penalties less than 300

R^2	0.82					
	coefficient	standard error	t	p-value	[0.025	0.975]
const	2.51	0.262	9.607	0.000	1.979	3.049
LJ_{p1}	0.63	0.288	2.204	0.036	0.046	1.222
LJ_{p2}	-5.80	1.317	-4.406	0.000	-8.497	-3.109
LJ_{p3}	4.92	1.222	4.027	0.000	2.421	7.419
LJ_{std}	3.49	0.773	4.52	0.000	1.912	5.074
$Coul_{p1}$	-0.01	0.001	-4.072	0.000	-0.009	-0.003
$Coul_{p2}$	0.03	0.009	3.336	0.002	0.012	0.051
$Coul_{p3}$	-0.03	0.009	-2.779	0.009	-0.045	-0.007

$Coul_{std}$	-0.04	0.006	-6.235	0.000	-0.05	-0.025
W LJ_{p2}	0.21	0.052	4.025	0.000	0.103	0.317
W LJ_{p3}	-0.20	0.052	-3.843	0.001	-0.307	-0.094
W LJ_{std}	0.35	0.08	4.45	0.000	0.192	0.518
S_W	0.14	0.063	2.163	0.039	0.007	0.265

REFERENCES

(1) Smith, J. N.; Flagan, R. C.; Beauchamp, J. L. Droplet Evaporation and Discharge Dynamics in Electrospray Ionization. *J. Phys. Chem. A* **2002**, *106* (42), 9957–9967. https://doi.org/10.1021/jp025723e.

(2) Maze, J. T.; Jones, T. C.; Jarrold, M. F. Negative Droplets from Positive Electrospray. *J. Phys. Chem. A* **2006**, *110* (46), 12607–12612. https://doi.org/10.1021/jp064581b.

(3) *IUPAC - Non-standard reduction potentials*. https://old.iupac.org/didac/Didac%20Eng/Didac03/Content/R10.htm (accessed 2024-05-23).

(4) Zoski, C. G. *Handbook of Electrochemistry*; Elsevier Science, 2007.